

Research Article

Other-Cell Interference Reducing Resource Allocation in OFDM-Based Asynchronous Cellular Systems

Jin-Woo Lee, June Moon, and Yong-Hwan Lee

School of Electrical Engineering and INMC, Seoul National University, P.O. Box 34, Kwanak, Seoul 151-600, South Korea

Correspondence should be addressed to Jin-Woo Lee, jinu@ttl.snu.ac.kr

Received 4 April 2007; Accepted 25 September 2007

Recommended by Hikmet Sari

Orthogonal frequency division multiplexing (OFDM) is considered as one of the most promising techniques for next-generation wireless access systems. However, it may suffer from the so-called other-cell interference (OCI) in cellular environments. In this paper, we consider a novel resource allocation scheme to reduce the OCI in OFDM-based asynchronous cellular systems. The proposed scheme can reduce the OCI by exploiting repetitive properties of cyclic prefix of OFDM symbol and asynchronous properties between the user and the base stations in other cells. The proposed scheme can be applied to various types of OFDM-based systems such as orthogonal frequency division multiple access (OFDMA) and multicarrier code division multiple access (MC-CDMA) systems. Simulation results show that the proposed scheme can reduce the OCI by nearly up to 1 dB compared to conventional schemes, yielding an increase of the throughput of about 15% near the cell boundary in OFDM-based asynchronous cellular environments.

Copyright © 2008 Jin-Woo Lee et al. This is an open access article distributed under the Creative Commons Attribution License, which permits unrestricted use, distribution, and reproduction in any medium, provided the original work is properly cited.

1. INTRODUCTION

Broadband wireless packet access systems have attracted for the achievement of high-speed transmission capacity. Orthogonal frequency division multiplexing (OFDM) is known as one of the best transmission techniques for this purpose due to the simplicity of channel equalization even in severely frequency selective wireless channel by converting wideband frequency selective fading into a series of narrowband flat fading [1–3]. However, it may suffer from other-cell interference (OCI) in cellular environments that use the same frequency band for all cells [4]. As a consequence, the system capacity is mainly limited by the OCI rather than other noise in interference-limited environments.

A number of researches have been reported on the mitigation of OCI. They can be classified basically into two categories according to the mitigation strategy of OCI: OCI averaging and OCI avoidance. OCI averaging schemes require a simple transceiver structure and can easily control the radio resource with the aid of spread spectrum and/or frequency hopping (FH) techniques [5, 6]. These techniques have been exploited in multicarrier code division multiple access (MC-CDMA) [7] and frequency hopping orthogonal frequency division multiple access (FH-OFDMA) sys-

tems [8]. They can provide a diversity gain as a result of channel and/or OCI averaging effect. However, the performance of MC-CDMA and FH-OFDMA systems is typically limited by the amount of average OCI. As a result, they may not provide significant performance improvement in cellular environments. On the other hand, OCI avoidance schemes can reduce the interference by dynamically avoiding adjacent base stations (BSs) to use the same frequency resource used by the target BS. Dynamic packet assignment (DPA) [9] and fractional frequency reuse (FFR) [10, 11] are typical examples of OCI avoidance schemes. However, OCI avoidance schemes require a large amount of additional information exchange among the BSs through backbone networks. What is worse, they may not be applicable to OFDM-based asynchronous cellular systems due to inherited timing difference among the BSs [12].

In this paper, we propose a novel resource allocation scheme that can reduce the OCI in OFDM-based asynchronous cellular systems. By reducing the power of the last portion of the OFDM symbol used as the cyclic prefix (CP), the proposed resource allocation scheme can noticeably reduce the OCI. The proposed scheme can easily be applied to OFDMA [13] and MC-CDMA systems [3], providing significant throughput improvement near the cell boundary.

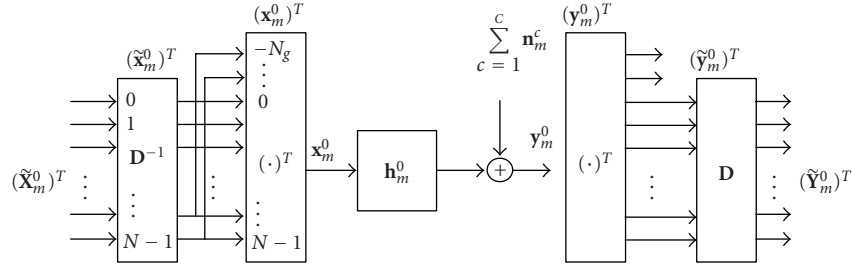


FIGURE 1: OFDM system model.

The remainder of this paper is organized as follows. Section 2 describes the system model in consideration. In Section 3, the proposed OCI reducing scheme is described. Then, the proposed resource allocation methods are applied to OFDM-based cellular systems in Section 4. The performance of the proposed schemes is verified by computer simulation in Section 5. Finally, conclusions are summarized in Section 6.

2. SYSTEM MODEL

Consider the transmission of the m th OFDM symbol matrix from the 0th cell (i.e., the target BS), which is defined by $\tilde{\mathbf{X}}_m^0 = [(\tilde{X}_m^0)_0 \cdots (\tilde{X}_m^0)_{N-1}]$ in the frequency domain. Figure 1 illustrates the discrete time OFDM system model in consideration. The OFDM transmitter converts $\tilde{\mathbf{X}}_m^0$ into a time domain OFDM symbol matrix $\tilde{\mathbf{X}}_m^0 = [(\tilde{X}_m^0)_0 \cdots (\tilde{X}_m^0)_{N-1}]$ by the inverse discrete Fourier transform (IDFT) \mathbf{D}^{-1} as

$$\left(\tilde{\mathbf{x}}_m^0\right)^T = \mathbf{D}^{-1} \left(\tilde{\mathbf{X}}_m^0\right)^T, \quad (1)$$

where \mathbf{a}^T and \mathbf{a}^{-1} , respectively, denote the transpose, inverse of matrix \mathbf{a} , and \mathbf{D} is an $(N \times N)$ discrete Fourier transform (DFT) matrix defined by [14]

$$\mathbf{D} \triangleq \frac{1}{\sqrt{N}} \begin{bmatrix} 1 & 1 & \cdots & 1 \\ 1 & e^{-j2\pi 1 \cdot 1/N} & \cdots & e^{-j2\pi 1 \cdot (N-1)/N} \\ \vdots & \vdots & \ddots & \vdots \\ 1 & e^{-j2\pi (N-1) \cdot 1/N} & \cdots & e^{-j2\pi (N-1) \cdot (N-1)/N} \end{bmatrix}. \quad (2)$$

Here, N denotes the number of subcarriers (i.e., the OFDM symbol duration in the sample time domain) and $j = \sqrt{-1}$.

To mitigate the intersymbol interference (ISI) and intercarrier interference (ICI) due to multipath delay spread, a CP which is a replica of the last portion of the OFDM symbol is inserted at the beginning of each OFDM symbol as [1]

$$\mathbf{x}_m^0 = \left[\left(\tilde{\mathbf{x}}_m^0\right)_{\{(N-N_g):(N-1)\}} \tilde{\mathbf{x}}_m^0 \right], \quad (3)$$

where $\mathbf{a}_{\{n_1:n_2\}} \triangleq [a_{n_1} \cdots a_{n_2}]$ and N_g is the CP duration in the sample time domain. Assume that the channel impulse response matrix $\mathbf{h}_m^0 = [(h_{m-N_g}^0) \cdots (h_m^0)_{N-1}]$ affects the

signal \mathbf{x}_m^0 only by the path-loss propagation (i.e., all the elements of \mathbf{h}_m^0 are equal to $1/(r_0)^{\alpha/2}$, where r_0 is the distance between the transceivers in the 0th cell, and α denotes the path-loss exponent). Then, the m th received OFDM symbol matrix including the CP from the 0th cell can be represented as

$$\begin{aligned} \mathbf{y}_m^0 &= \mathbf{h}_m^0 \times \mathbf{x}_m^0 + \sum_{c=1}^C \mathbf{n}_m^c \\ &= \mathbf{x}_m^0 / (r_0)^{\alpha/2} + \sum_{c=1}^C \mathbf{n}_m^c, \end{aligned} \quad (4)$$

where $\mathbf{n}_m^c = [(n_{m-N_g}^c) \cdots (n_{m-1}^c)]$ denotes the OCI from the c th cell, C is the number of other cells, and symbol “ \times ” denotes group direct product defined by $\mathbf{a} \times \mathbf{b} \triangleq [a_1 b_1 \cdots a_N b_N]$ when $\mathbf{a} = [a_1 \cdots a_N]$ and $\mathbf{b} = [b_1 \cdots b_N]$.

The m th received OFDM symbol matrix $\tilde{\mathbf{y}}_m^0$ from the 0th cell can be obtained by discarding the first N_g samples (i.e., the CP) of \mathbf{y}_m^0 as

$$\tilde{\mathbf{y}}_m^0 = \left(\mathbf{y}_m^0\right)_{\{0:(N-1)\}}. \quad (5)$$

Then, it is demodulated by DFT as

$$\left(\tilde{\mathbf{Y}}_m^0\right)^T = \mathbf{D} \left(\tilde{\mathbf{y}}_m^0\right)^T, \quad (6)$$

where \mathbf{D} denotes a DFT processor.

Since the OCI from other cells is not synchronized with the signal from the 0th cell in an OFDM-based asynchronous cellular system, it can be represented as

$$\begin{aligned} &\sum_{c=1}^C \mathbf{n}_m^c \\ &= \sum_{c=1}^C \{[(\mathbf{x}_{m-1}^c)_{\{(N+N_g-\Delta_c):(N-1)\}} (\mathbf{x}_m^c)_{\{-N_g:(N-1-\Delta_c)\}}] / (r_c)^{\alpha/2}\}, \end{aligned} \quad (7)$$

where Δ_c denotes the timing offset between the 0th cell and the c th cell. Figure 2 illustrates the shape of asynchronization between the OCI and the desired signal.

3. CONCEPT OF THE PROPOSED OCI REDUCTION

A CP is inserted at the beginning of each OFDM symbol to mitigate the ISI and ICI due to the multipath delay spread in

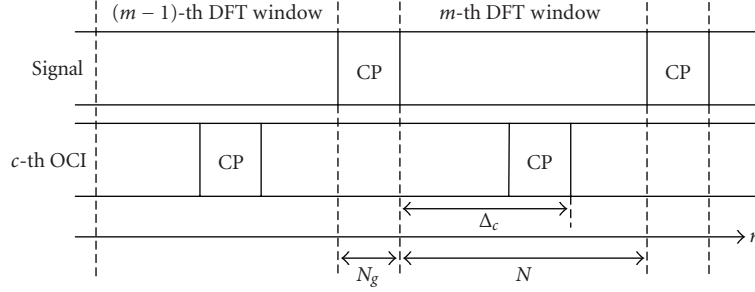


FIGURE 2: OCI distribution in OFDM-based asynchronous cellular systems.

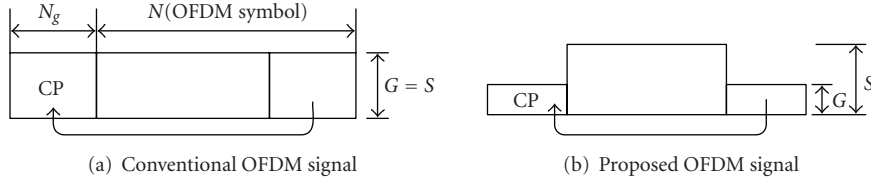


FIGURE 3: The concept of signal power reduction.

OFDM systems. Since the CP itself is a redundancy requiring additional power, it may be desirable to reduce the power of the CP. If the power of the CP can be reduced, the average transmit power can be reduced and thus the power of OCI to other users can also be reduced in an OFDM-based asynchronous cellular system.

In a conventional OFDM system, the CP is generated as a replica of the last portion of the OFDM symbol with the same power and thus it has the same average transmit power as the rest of OFDM symbol, as illustrated in Figure 3(a). To reduce the power of the CP, it is required to design the OFDM symbol to have lower power in its last portion corresponding to the CP. Figure 3(b) illustrates the design of OFDM symbols for the proposed scheme.

As illustrated in Figure 3, let G and S be the average power of the last portion of the OFDM symbol corresponding to the CP and the rest of the OFDM symbol, respectively, as

$$G = \frac{1}{N_g} \left\| (\mathbf{x}_m^c)_{\{-N_g:-1\}} \right\|^2 = \frac{1}{N_g} \left\| (\mathbf{x}_m^c)_{\{(N-N_g):(N-1)\}} \right\|^2$$

$$S = \frac{1}{N - N_g} \left\| (\mathbf{x}_m^c)_{\{0:(N-N_g-1)\}} \right\|^2, \quad (8)$$

where $\|\mathbf{a}\|$ denotes the Euclidean norm of \mathbf{a} . Thus, the average OCI power from the c th cell can be represented as

$$P_c = \frac{N_g G + (N - N_g) S}{N} \frac{1}{(r_c)^\alpha}. \quad (9)$$

Thus, the total average OCI power can be represented as

$$P = \sum_{c=1}^C P_c = \frac{N_g G + (N - N_g) S}{N} \sum_{c=1}^C \frac{1}{(r_c)^\alpha}. \quad (10)$$

Figure 4 illustrates the signal distribution when the proposed signaling is applied to an asynchronous OFDM cellular system. Since the signals from the target BS are synchronized to the desired signal, the power reduction of the last portion of the OFDM symbol corresponding to the CP does not affect the reception performance. However, it can be seen that the average OCI power from other BSs is reduced in the presence of symbol timing misalignment between the transceivers in this asynchronous cellular system. (In an OFDM-based synchronous cellular system, on the other hand, the OCI reduction gain cannot be achieved since the power reduced CP of OCI at the outside of the DFT window is also perfectly removed as that of signal from the intra BS (i.e., $P = P'$ when $0 \leq \Delta_c < N_g$.)

The average OCI power from the c th cell can be represented as

$$P'_c(\Delta_c) = \frac{1}{N} E \left\{ \left\| [(\mathbf{x}_{m-1}^c)_{\{(N+N_g-\Delta_c):(N-1)\}} (\mathbf{x}_m^c)_{\{-N_g:(N-1-\Delta_c)\}}] \right\|^2 \right\} \frac{1}{(r_c)^\alpha}$$

$$= \begin{cases} \frac{N_g G + (N - N_g) S}{N} \frac{1}{(r_c)^\alpha}, & 0 \leq \Delta_c < N_g \\ \frac{\Delta_c G + (N - \Delta_c) S}{N} \frac{1}{(r_c)^\alpha}, & N_g \leq \Delta_c < 2N_g \\ \frac{2N_g G + (N - 2N_g) S}{N} \frac{1}{(r_c)^\alpha}, & 2N_g \leq \Delta_c < N \\ \frac{(N + 2N_g - \Delta_c) G + (\Delta_c - 2N_g) S}{N} \frac{1}{(r_c)^\alpha}, & N \leq \Delta_c < N_g + N, \end{cases} \quad (11)$$

where $E\{a\}$ denotes the expectation of a . Since Δ_c is slowly varying due to the propagation delay between the two

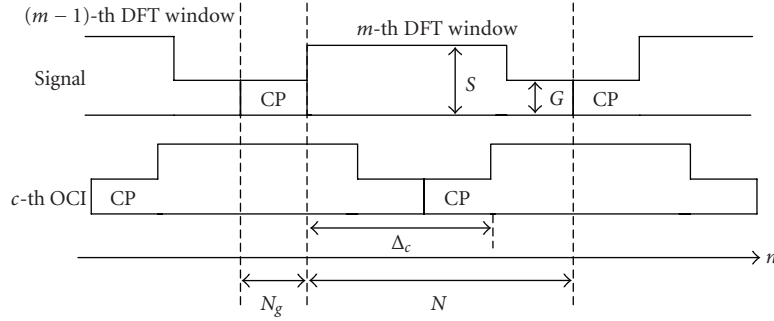


FIGURE 4: Reduced OCI power in OFDM-based asynchronous cellular systems.

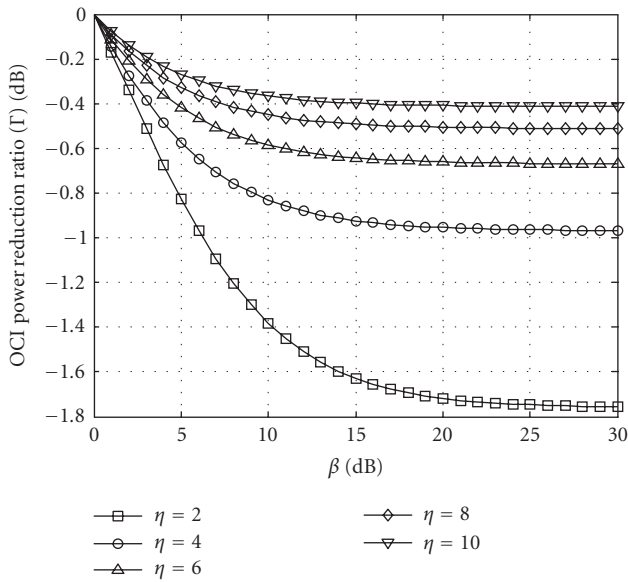


FIGURE 5: The average OCI power reduction ratio as a function of η and β .

transceivers, it can be assumed that Δ_c is uniformly distributed. Then, the average OCI power is changed by the proposed scheme as

$$P'_c = E_{\Delta_c} \{P'_c(\Delta_c)\} = \frac{2N_g G + (N - N_g)S}{(N + N_g)} \frac{1}{(r_c)^\alpha} \quad (12)$$

and the total average OCI power becomes as

$$P' = \sum_{c=1}^C P'_c = \left\{ \frac{2N_g G + (N - N_g)S}{(N + N_g)} \right\} \sum_{c=1}^C \frac{1}{(r_c)^\alpha}. \quad (13)$$

Note that the average power of the OCI in the conventional scheme is P . Letting η be the ratio of the OFDM symbol duration to the CP duration (i.e., $\eta = N/N_g$) and β the ratio of the average OFDM symbol power to the average CP symbol power (i.e., $\beta = S/G$), define the OCI power reduction ratio by

$$\Gamma \triangleq \frac{P'}{P} = \frac{\eta}{\eta + 1} \left(1 + \frac{1}{1 + (\eta - 1)\beta} \right). \quad (14)$$

Figure 5 depicts the amount of OCI power reduction according to the values of η and β . It can be seen that the gain of the proposed scheme over the conventional one increases as η decreases and/or β increases. In practice, η is designed by considering the maximum delay and Doppler spread [15]. For example, $\eta = 4$ in the radio access system in [16] and $\eta = 8$ in the mobile WiMAX system in [17]. Since η is a fixed parameter in practice, the performance can be improved by increasing β .

4. PROPOSED RESOURCE ALLOCATION FOR MULTIUSER OFDM SYSTEMS

In this Section, we propose a novel resource allocation rule to increase β in multiuser OFDM systems such as OFDMA system and MC-CDMA system. Unless all the resources (e.g., subcarriers in the OFDMA and spreading codes in the MC-CDMA) of multiuser OFDM systems are fully utilized for the signal transmission (i.e., no room for the signal design with increased β), we can reduce the power of the CP by exploiting the proposed resource allocation scheme.

4.1. OFDMA system

The OFDMA divides the whole frequency band into multiple subcarriers and assigns subcarriers to each user at an OFDM symbol time. It supports flexible data transmission by formatting the digital modulation on each subcarrier.

4.1.1. Optimum subcarrier allocation

To maximize β (i.e., to minimize the average power of the last portion of the time domain OFDM symbol $\tilde{\mathbf{x}}_m^c$), we exploit the reciprocal characteristics between the time domain and the frequency domain. In what follows, the subscript m and the superscript c of $\tilde{\mathbf{x}}_m^c$ are omitted for simplicity of description.

Assume that there are U users. Then, $\tilde{\mathbf{X}}$ can be represented as

$$\begin{aligned} \tilde{\mathbf{X}} &= [\tilde{X}_0 \ \cdots \ \tilde{X}_{N-1}] \\ &= \mathbf{w} [b_0 \ \cdots \ b_{U-1} \ v_0 \ \cdots \ v_{N-U-1}] \\ &= \mathbf{w} [\mathbf{b} \ \mathbf{v}], \end{aligned} \quad (15)$$

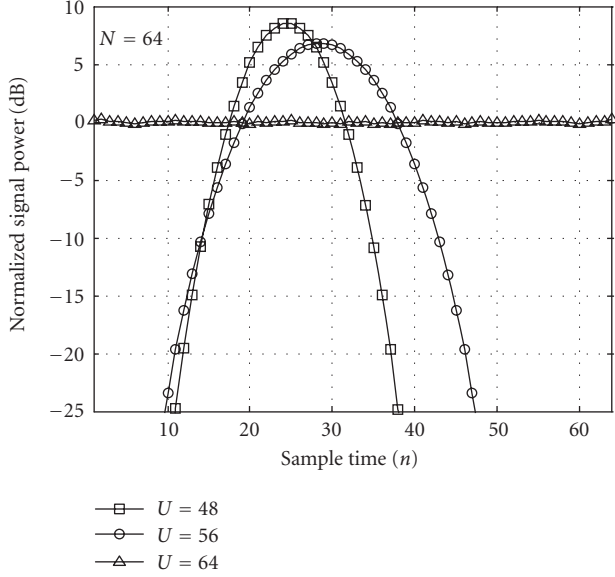


FIGURE 6: Power of the proposed optimum OFDMA signal when $N = 64$.

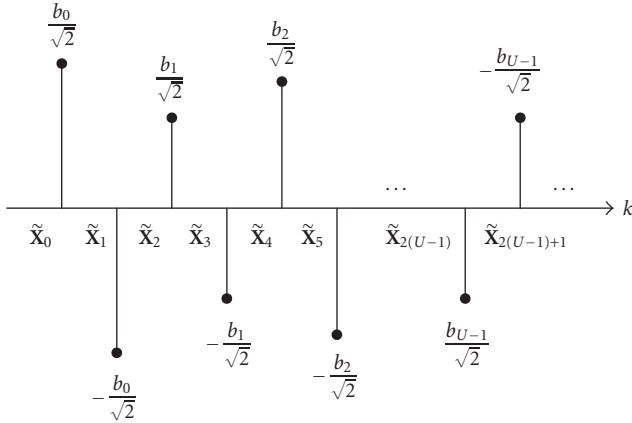


FIGURE 7: The proposed suboptimum resource allocation scheme.

where w is a weighting constant for the power normalization determined as

$$w = \sqrt{\frac{\|\mathbf{b}\|^2}{\|\mathbf{b}\|^2 + \|\mathbf{v}\|^2}}, \quad (16)$$

\mathbf{b} is the data symbol matrix of U users, and \mathbf{v} is a redundant signal matrix to be designed to make the last portion of the time domain OFDM symbol $\tilde{\mathbf{x}}$ zero as

$$\tilde{\mathbf{x}} = [\tilde{\mathbf{x}}_1 \ \tilde{\mathbf{x}}_2] = [\tilde{\mathbf{x}}_1 \ 0]. \quad (17)$$

Here $\tilde{\mathbf{x}}_1 = \tilde{\mathbf{x}}_{\{0:(U-1)\}}$ and $\tilde{\mathbf{x}}_2 = \tilde{\mathbf{x}}_{\{U:(N-1)\}} = \mathbf{0}$.

Decompose \mathbf{D} into four partial matrices as

$$\mathbf{D} = \begin{bmatrix} \mathbf{D}_1 & \mathbf{D}_2 \\ \mathbf{D}_3 & \mathbf{D}_4 \end{bmatrix}, \quad (18)$$

where \mathbf{D}_1 is a $(U \times U)$ matrix, \mathbf{D}_2 is a $(U \times (N - U))$ matrix, \mathbf{D}_3 is a $((N - U) \times U)$ matrix, and \mathbf{D}_4 is a $((N - U) \times (N - U))$ matrix. Then, we have

$$\begin{aligned} (\tilde{\mathbf{X}})^T &= \mathbf{D}(\tilde{\mathbf{x}})^T, \\ w[\mathbf{b} \ \mathbf{v}]^T &= \begin{bmatrix} \mathbf{D}_1 & \mathbf{D}_2 \\ \mathbf{D}_3 & \mathbf{D}_4 \end{bmatrix} [\tilde{\mathbf{x}}_1 \ 0]^T. \end{aligned} \quad (19)$$

Since

$$w(\mathbf{b})^T = \mathbf{D}_1(\tilde{\mathbf{x}}_1)^T, \quad (20)$$

$(\tilde{\mathbf{x}}_1)^T$ can be obtained by

$$(\tilde{\mathbf{x}}_1)^T = w\mathbf{D}_1^{-1}(\mathbf{b})^T. \quad (21)$$

Since

$$w(\mathbf{v})^T = \mathbf{D}_3(\tilde{\mathbf{x}}_1)^T, \quad (22)$$

\mathbf{v} can be designed by

$$\mathbf{v} = \mathbf{b}(\mathbf{D}_1^{-1})^T(\mathbf{D}_3)^T. \quad (23)$$

Let $m_F(k)$ be the data symbol allocated to the k th subcarrier. Then, the subcarrier for the OFDMA signal can be allocated as

$$m_F(k) = \begin{cases} wb_k, & k = 0, 1, \dots, U - 1, \\ wv_{k-U}, & k = U, U + 1, \dots, N. \end{cases} \quad (24)$$

Note that, when $U \leq N - N_g$, it can be possible to make β infinite by making the average power G of the CP zero. Figure 6 depicts the average signal power of the proposed OFDMA signal for different values of U when $N = 64$. It can be seen that the power of the last portion of the signal can perfectly be controlled when $U \leq N - N_g$. When $U > N - N_g$, the resource will be allocated to the last portion of the OFDM symbol in the time domain, yielding somewhat performance degradation.

4.1.2. Suboptimum subcarrier allocation

Although the optimum subcarrier allocation rule can provide significant performance improvement, it may not be applicable in practice due to the implementation complexity. Thus, we consider a simple subcarrier allocation rule to increase β in multiuser OFDMA environments.

The proposed scheme allocates each pair of data symbols to the adjacent subcarriers with opposite signs as illustrated in Figure 7. Let $m_F(k)$ be the data symbol allocated to the

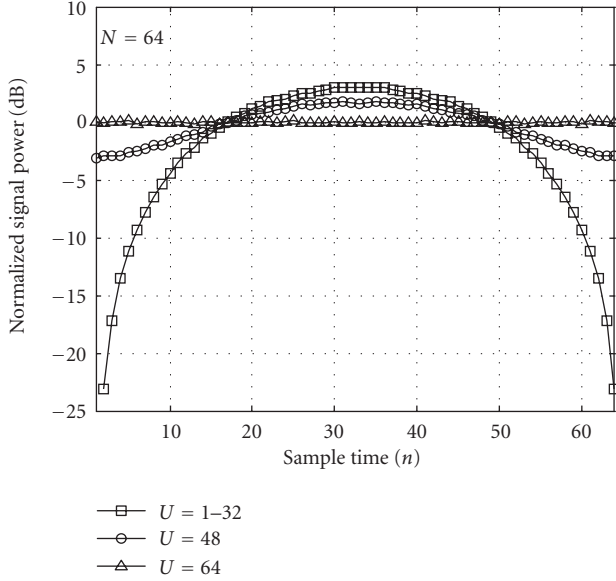


FIGURE 8: Power of the proposed suboptimum OFDMA signal when $N = 64$.

k th subcarrier. Then, the subcarrier for the OFDMA signal can be allocated as

$$m_F(k) = \begin{cases} b_{k/2}/\sqrt{2}, & k = 0, 2, \dots, 2(U-1) \\ -b_{(k-1)/2}/\sqrt{2}, & k = 1, 3, \dots, 2(U-1)+1 \\ \end{cases} \quad \text{when } U \leq N/2$$

$$= \begin{cases} b_{k/2}, & k = 0, 2, \dots, 2(U-N/2-1) \\ b_{N/2+k}, & k = 1, 3, \dots, 2(U-N/2-1)+1 \\ b_{k/2}/\sqrt{2}, & k = 2(U-N/2), \dots, 2(N/2-1) \\ -b_{(k-1)/2}/\sqrt{2}, & k = 2(U-N/2)+1, \dots, \\ & 2(N/2-1)+1, \\ \end{cases} \quad \text{when } U > N/2. \quad (25)$$

Note that when $U \leq N/2$, each pair of symbols allocated to the adjacent subcarriers will have opposite signs. However, when $U > N/2$, $(U - N/2)$ pairs of symbols allocated to the adjacent subcarriers do not have opposite signs. The proposed resource allocation rule generates an OFDM signal that has a \cap -shaped power characteristic in the time domain as shown in Figure 8 (refer to the appendix). Thus, the proposed scheme can increase β compared to conventional schemes, reducing the average OCI power without the increase of complexity.

Figure 8 depicts the average signal power of the proposed OFDMA signal for different values of U when $N = 64$. It can be seen that the OFDM signal has a \cap -shaped power char-

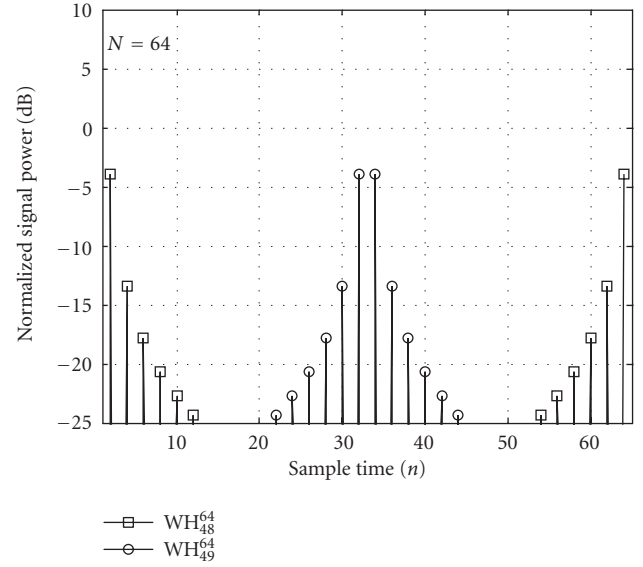


FIGURE 9: Power of the proposed suboptimum MC-CDMA signal with WH spreading code when $N = 64$.

acteristic and the average signal power corresponding to the CP is noticeably reduced when $U \leq N/2$.

4.2. MC-CDMA system

The MC-CDMA system transmits multiuser signals by using orthogonal spreading codes. The use of spreading codes can reduce the fluctuation of channel and/or interference, yielding a diversity gain.

4.2.1. Optimum WH code allocation

Real-valued binary codes (e.g., Walsh-Hadamard (WH) codes) are often employed as the spreading code due to their simplicity [18]. If the spreading factor L is equal to N , there can exist N spreading codes. The WH code can optimally be allocated for the reduction of β by exhaustive search using the spectral properties of the WH code [19].

4.2.2. Suboptimum WH code allocation

The optimum WH code allocation rule can significantly reduce the OCI. However, it may not easily be realizable because it is associated with the values of N and η . Thus it may be desirable to employ a suboptimum allocation rule robust to the variation of these parameters.

The WH codes have a property that each pair of adjacent chips with an odd index and an even index has opposite signs and the same signs, respectively. For example, WH codes of length 4 can be represented as $WH_0^4 = \{1, 1, 1, 1\}$, $WH_1^4 = \{1, -1, 1, -1\}$, $WH_2^4 = \{1, 1, -1, -1\}$, $WH_3^4 = \{1, -1, -1, 1\}$, where WH_k^l denotes the k th WH code of length l . As illustrated in Figure 9, the WH codes with an odd index make the OFDM signal with a \cap -shaped power characteristic. Thus,

the WH spreading codes with an odd index have preference for the allocation over those with an even index.

When a WH code is used as the spreading code, the resource can be allocated for the MC-CDMA system as

$$m_{\text{WH}}(k) = \begin{cases} b_{(k-1)/2}, & k = 1, 3, \dots, 2U - 1, \\ & \text{when } U \leq N/2 \\ b_{(k-1)/2}, & k = 1, 3, \dots, N - 1 \\ b_{(N+k)/2}, & k = 0, 2, \dots, 2(U - N/2 - 1), \\ & \text{when } U > N/2 \end{cases} \quad (26)$$

where $m_{\text{WH}}(k)$ denotes the data symbol allocated to the k th WH spreading code of length N (i.e., WH_k^N).

4.2.3. Optimum DFT code allocation

The OCI can further be reduced by employing a DFT basis as the spreading code. Let $\text{DFT}_k^l = e^{-j2\pi kn/l}$ be the k th spreading code of length l [20]. Since the IDFT of DFT_k^N is an impulse function located at time k as depicted in Figure 10, the MC-CDMA signal can be allocated using a DFT spreading code as

$$m_{\text{DFT}}(k) = b_k, \quad k = 0, 1, \dots, U - 1, \quad (27)$$

where $m_{\text{DFT}}(k)$ denotes the data symbol allocated to the k th DFT spreading code of length N . Thus, the power loss due to the CP can completely be eliminated when $U \leq N - N_g$ as depicted in Figure 10, yielding substantial reduction of the OCI power.

5. PERFORMANCE EVALUATION

The performance of the proposed resource allocation schemes is verified by computer simulation. Figure 11 depicts the OCI power reduction ratio Γ as a function of the number of users when $N = 64$ and $\eta = 4$. It can be seen that the proposed resource allocation schemes noticeably reduce the OCI unless U is too large. When applied to an OFDMA system, the proposed optimum allocation scheme reduces the OCI by nearly up to 1 dB when $U \leq N - N_g$. When $U > N - N_g$, the resource will be allocated to the last portion of the OFDM symbol in the time domain, yielding performance degradation. The proposed suboptimum allocation scheme provides a power reduction gain of nearly up to 0.6 dB when $U \leq N/2$. When $U > N/2$, Γ increases as U increases because $(U - N/2)$ pairs of symbols allocated to the adjacent subcarriers have the same signs. When applied to an MC-CDMA with the use of WH codes, the proposed optimum WH code allocation scheme provides an OCI power reduction of nearly up to 1 dB when U is very small. In addition, the proposed suboptimum WH code allocation scheme provides an OCI power reduction of nearly up to 0.6 dB. It can be seen that

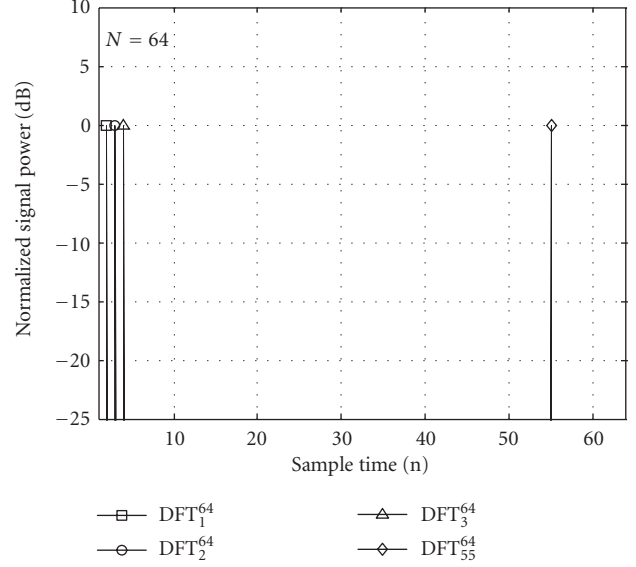


FIGURE 10: Power of the proposed optimum MC-CDMA signal with DFT code when $N = 64$.

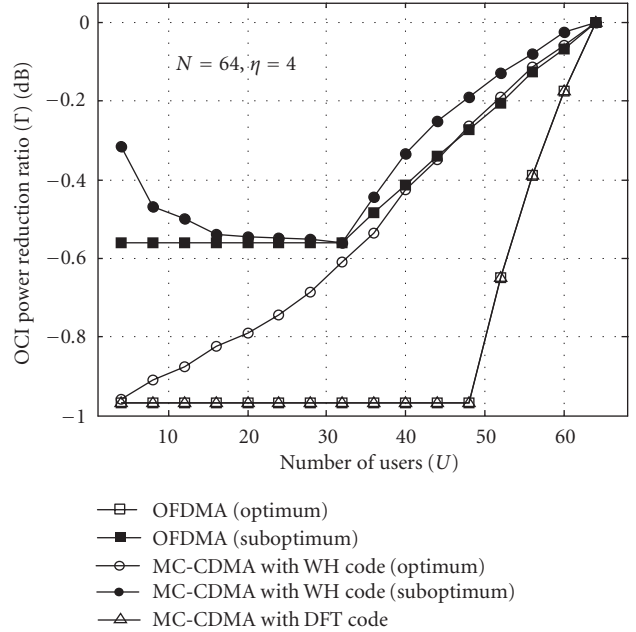


FIGURE 11: The average OCI power reduction associated with U .

the MC-CDMA with the use of DFT spreading codes provides performance better than the use of WH codes. The proposed scheme provides an OCI reduction of nearly 1 dB with the use of DFT code when $U \leq N - N_g$ since β is infinite (i.e., $\Gamma_{\beta \rightarrow \infty} = \eta/(\eta + 1)$). When $U > N - N_g$, the resource will be allocated to the last portion of the OFDM symbol in the time domain, yielding substantial performance degradation.

Figure 12 depicts the average throughput of users near the cell boundary (i.e., $0.8 < r_0 \leq 1$ km) when $N = 64$

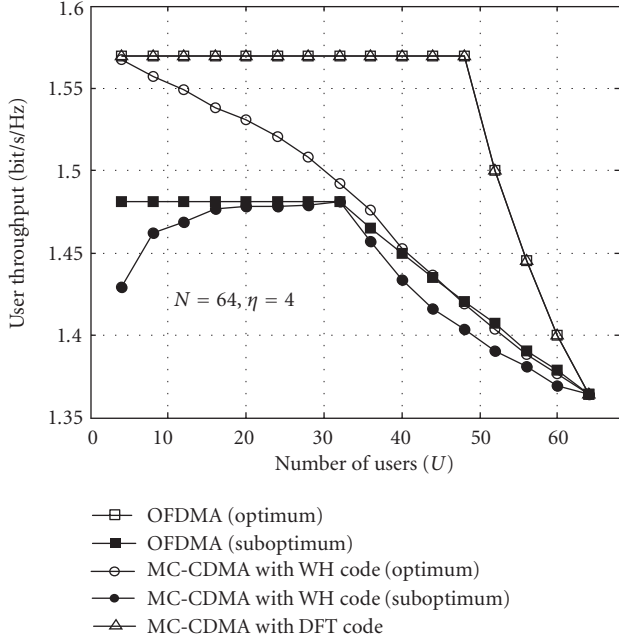


FIGURE 12: The average user throughput near the cell boundary in a 19-cell configuration.

and $\eta = 4$. Here, we assume that 19-cell configuration with cell radius $R = 1$ km and path loss exponent $\alpha = 4$ as considered in [21]. It can be seen that when applied to an OFDMA system, the proposed scheme can increase the average throughput of users near the cell boundary by nearly up to 0.21 bit/s/Hz (or increase of the average throughput by approximately 15%) when $U \leq N - N_g$. It can also be seen that when applied to an MC-CDMA with the use of DFT spreading codes, the proposed scheme can increase the average throughput of users near the cell boundary by nearly 0.21 bit/s/Hz. This implies the effectiveness of OCI reduction near the cell boundary.

6. CONCLUSIONS

We have proposed novel resource allocation schemes that can reduce the OCI in OFDM-based asynchronous cellular systems by reducing the power of the last portion of the OFDM symbol, corresponding to the power of the CP. The proposed resource schemes can easily be applied to OFDMA and MC-CDMA systems. Simulation results show that the proposed schemes can reduce the OCI power by nearly up to 1 dB, yielding an increase of the throughput of users near the cell boundary by about 15% in MC-CDMA- and OFDMA-based cellular environments. Notice that there may be a slight increase of the peak-to-average power ratio (PAPR) due to the use of unequal power for the OFDM signal generation. Further consideration may need to optimize the OCI reduction without noticeable increase of the PAPR.

APPENDIX

A. CHARACTERISTICS OF THE PROPOSED SUBOPTIMUM OFDMA SIGNAL

We prove that the proposed suboptimum resource allocation scheme generates an OFDMA signal with a \cap -shaped power characteristic. When $U \leq N/2$, \tilde{X}_k (i.e., $m_F(k)$) can be decomposed into two terms by the proposed suboptimum allocation method (25), \tilde{X}_n^e and \tilde{X}_n^o , with odd and even indices as

$$\begin{aligned} \tilde{X}_k^e &= \begin{cases} b_{k/2}/\sqrt{2}, & \text{even } k, \\ 0, & \text{odd } k, \end{cases} \\ \tilde{X}_k^o &= \begin{cases} 0, & \text{even } k, \\ -b_{(k-1)/2}/\sqrt{2}, & \text{odd } k. \end{cases} \end{aligned} \quad (\text{A.1})$$

Then, the time domain signal can be obtained by the IDFT operation as

$$\begin{aligned} \tilde{x}_n &= \frac{1}{\sqrt{N}} \sum_{k=0}^{N-1} \tilde{X}_k e^{j2\pi nk/N} \\ &= \frac{1}{\sqrt{N}} \sum_{k=0}^{N-1} (\tilde{X}_k^e + \tilde{X}_k^o) e^{j2\pi nk/N}, \end{aligned} \quad (\text{A.2})$$

where n is the sample time index of the OFDM symbol. Since $\tilde{X}_k^o = -\tilde{X}_{k-1}^e$, (A.2) can be rewritten as

$$\begin{aligned} \tilde{x}_n &= \frac{1}{\sqrt{N}} \sum_{k=0}^{N-1} (\tilde{X}_k^e - \tilde{X}_{k-1}^e) e^{j2\pi nk/N} \\ &= \frac{1}{\sqrt{N}} (1 - e^{j2\pi n/N}) \sum_{k=0}^{N-1} \tilde{X}_k^e e^{j2\pi nk/N}. \end{aligned} \quad (\text{A.3})$$

The average power at symbol time n can be obtained by

$$P_{x_n} = E\{|\tilde{x}_n|^2\} = AS_n, \quad (\text{A.4})$$

where

$$\begin{aligned} A &= \frac{1}{N} E\left\{ \left| \sum_{k=0}^{N-1} \tilde{X}_k^e e^{j2\pi nk/N} \right|^2 \right\}, \\ S_n &= |1 - e^{j2\pi n/N}|^2. \end{aligned} \quad (\text{A.5})$$

Note that A is a constant indifferent from the time index n in an average sense. Thus, the shape of P_{x_n} depends only on that of S_n . Since S_n has a \cap -shape, P_{x_n} also has a \cap -shape. Note that β can be obtained by

$$\beta = \frac{N_g}{N - N_g} \frac{\sum_{n=0}^{N-N_g-1} S_n}{\sum_{n=N-N_g}^{N-1} S_n}. \quad (\text{A.6})$$

ACKNOWLEDGMENT

This work was in part supported by Seoul R&BD Program (10544).

REFERENCES

- [1] R. van Nee and R. Prasad, *OFDM for Wireless Multimedia Communications*, Artech House, Boston, Mass, USA, 2000.
- [2] J. A. C. Bingham, "Multicarrier modulation for data transmission: an idea whose time has come," *IEEE Communications Magazine*, vol. 28, no. 5, pp. 5–14, 1990.
- [3] S. Hara and R. Prasad, "Overview of multicarrier CDMA," *IEEE Communications Magazine*, vol. 35, no. 12, pp. 126–133, 1997.
- [4] T. S. Rappaport, *Wireless Communications*, Prentice-Hall, Upper Saddle River, NJ, USA, 1996.
- [5] S. Haykin, *Communication Systems*, John Wiley & Sons, New York, NY, USA, 2001.
- [6] J. G. Proakis, *Digital Communications*, McGraw-Hill, New York, NY, USA, 2001.
- [7] S. Kaiser, "OFDM code-division multiplexing in fading channels," *IEEE Transactions on Communications*, vol. 50, no. 8, pp. 1266–1273, 2002.
- [8] Flarion, "The benefits of a packet-switched, ALL-IP mobile broadband network," Flarion white paper, February 2004.
- [9] J. C. Chuang and N. R. Sollenberger, "Dynamic packet assignment for advanced cellular Internet service," in *Proceedings of the IEEE Global Telecommunications Conference (GLOBECOM '97)*, vol. 3, pp. 1596–1600, Phoenix, Ariz, USA, November 1997.
- [10] S. Faruque, "High capacity cell planning based on fractional frequency reuse with optimum trunking efficiency," in *Proceedings of the 48th IEEE Vehicular Technology Conference (VTC '98)*, vol. 2, pp. 1458–1460, Ottawa, Ontario, Canada, May 1998.
- [11] IEEE 802.20 WG, QFDD and QTDD: proposed draft air interface specification, October 2005.
- [12] 3GPP, "Physical layer aspects for evolved universal terrestrial radio access (UTRA)," TR 25.814 V7.0.0, June 2006.
- [13] J. Gross, I. Paoluzzi, H. Karl, and A. Wolisz, "Throughput study for a dynamic OFDM-FDMA system with inband signaling," *Proceedings of the 59th IEEE Vehicular Technology Conference (VTC '04)*, vol. 3, pp. 1787–1791, 2004.
- [14] A. V. Oppenheim, R. W. Schaffer, and J. R. Buck, *Discrete-Time Signal Processing*, Prentice-Hall Signal Processing Series, Prentice-Hall, Upper Saddle River, NJ, USA, 1999.
- [15] A. Hutter, "Design of OFDM systems for frequency-selective and time-variant channels," in *International Zurich Seminar on Access, Transmission, Networking, Broadband Communications*, pp. 39-1–39-6, Zurich, Switzerland, February 2002.
- [16] J. Moon, J.-Y. Ko, and Y.-H. Lee, "A framework design for the next-generation radio access system," *IEEE Journal on Selected Areas in Communications*, vol. 24, no. 3, pp. 554–564, 2006.
- [17] IEEE P802.16e, "Draft IEEE standard for local and metropolitan area networks," Std., September 2004.
- [18] S.-H. Tsai, Y.-P. Lin, and C.-C. J. Kuo, "MAI-free MC-CDMA systems based on Hadamard-Walsh codes," *IEEE Transactions on Signal Processing*, vol. 54, no. 8, pp. 3166–3179, 2006.
- [19] Q. Shi and M. Latva-aho, "Simple spreading code allocation scheme for downlink MC-CDMA," *Electronics Letters*, vol. 38, no. 15, pp. 807–809, 2002.
- [20] G. Rath and C. Guillemot, "Performance analysis and recursive syndrome decoding of DFT codes for bursty erasure recovery," *IEEE Transactions on Signal Processing*, vol. 51, no. 5, pp. 1335–1350, 2003.
- [21] Z. Lei, D. J. Goodman, and N. B. Mandayam, "Location-dependent other-cell interference and its effect on the uplink capacity of a cellular CDMA system," in *Proceedings of the 49th IEEE Vehicular Technology Conference (VTC '99)*, vol. 3, pp. 2164–2168, Houston, Tex, USA, May 1999.

EURASIP Journal on Audio, Speech, and Music Processing

<http://www.hindawi.com/journals/asmp/>

Special Issue on Intelligent Audio, Speech, and Music Processing Applications

Call for Papers

Future audio, speech, and music processing applications need innovative intelligent algorithms that allow for human/environmental-based interactive interfaces with surrounding devices/systems in real-world settings. The need exists to control, process, render, and playback/project sound signals for different platforms under a diverse range of listening environments. The presence of these intelligent audio, speech, and music processing applications will create an environment that is sensitive, adaptive, and responsive to the presence of users.

Generally, three areas of research are considered, namely, analysis, communication, and interaction. Analysis covers both preprocessing of sound signals and extraction of information from the environment. Communication covers the transmission path/network, coding techniques, and conversion between spatial audio formats. The final area involves intelligent interaction with the audio/speech/music environment based on the users' location, signal information, and acoustical environment.

This special issue includes a variety of intelligent devices and applications working together to create an integral audio experience/environment for the users. A vision of intelligent signal processing environments and applications can also be proposed and describe how new audio/speech/music applications can enhance everyday entertainment as well as human communication experiences.

Topics of interest include (but are not limited to):

- 3D and spatial audio
- Automotive audio
- Audio/speech installation
- Audio network
- Audio/speech delivery
- Audio/speech for mobile and handheld/wearable devices
- Environmental noise control active & passive
- Embedded audio/speech intelligence
- Intelligent speech communication
- Coding techniques
- Music processing
- Personal soundscape/personal audio space
- Speech enhancement
- New applications/domains

Authors should follow the EURASIP Journal on Audio, Speech, and Music Processing manuscript format described at the journal site <http://www.hindawi.com/journals/asmp/>. Prospective authors should

submit an electronic copy of their complete manuscript through the journal Manuscript Tracking System at <http://mts.hindawi.com/>, according to the following timetable:

Manuscript Due	January 1, 2008
First Round of Reviews	March 1, 2008
Publication Date	July 1, 2008

Guest Editors

Woon-Seng Gan, Digital Signal Processing Laboratory, School of Electrical and Electronic Engineering, Nanyang Technological University, 50 Nanyang Avenue, Singapore 639798; ewsgan@ntu.edu.sg

Sen M. Kuo, Department of Electrical Engineering, Northern Illinois University, DeKalb, IL 60115, USA; kuo@ceet.niu.edu

John H. L. Hansen, Department of Electrical Engineering, University of Texas at Dallas, Richardson, TX 75083, USA; john.hansen@utdallas.edu

RESEARCH LETTERS IN COMMUNICATIONS

Why publish in this journal?

Research Letters in Communications is devoted to very fast publication of short, high-quality manuscripts in the broad field of communications. The journal aims for a publication speed of 60 days from submission until final publication. Articles will be limited to a maximum of four published pages, and they should convey important results that have not been previously published.

Why publish in this journal?

Wide Dissemination

All articles published in the journal are freely available online with no subscription or registration barriers. Every interested reader can download, print, read, and cite your article

Quick Publication

The journal employs an online «Manuscript Tracking System» which helps streamline and speed the peer review so all manuscripts receive fast and rigorous peer review. Accepted articles appear online as soon as they are accepted, and shortly after, the final published version is released online following a thorough in-house production process.

Professional Publishing Services

The journal provides professional copyediting, typesetting, graphics, editing, and reference validation to all accepted manuscripts.

Keeping Your Copyright

Authors retain the copyright of their manuscript, which are published using the “Creative Commons Attribution License,” which permits unrestricted use of all published material provided that it is properly cited.

Extensive Indexing

Articles published in this journal will be indexed in several major indexing databases to ensure the maximum possible visibility of each published article.

Submit your Manuscript Now...

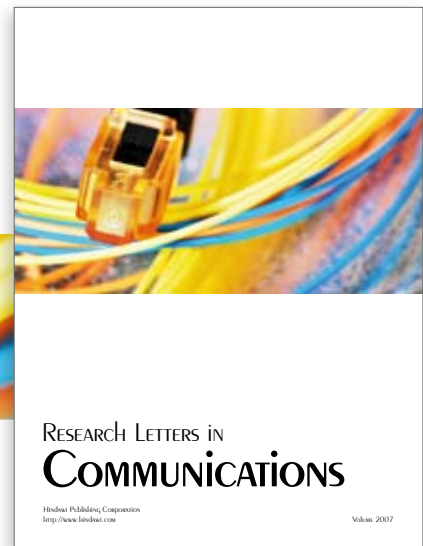
Please visit the journal’s website found at <http://www.hindawi.com/journals/rlc/> in order to submit your manuscript and click on the “Manuscript Submission” link in the navigational bar.

Should you need help or have any questions, please drop an email to the journal’s editorial office at rlc@hindawi.com

ISSN: 1687-6741; e-ISSN: 1687-675X; doi:10.1155/RLC

Hindawi Publishing Corporation
410 Park Avenue, 15th Floor, #287 pmb, New York, NY 10022, USA

HINDAWI



Editor-in-Chief

Maria-Gabriella Di Benedetto
Italy

Associate Editors

Huseyin Arslan
USA

E. K. S. Au

Hong Kong

Zhi Ning Chen

Singapore

René Cumplido

Mexico

Michele Elia

Italy

Lijia Ge

China

Amoakoh Gyasi-Agyei

Australia

Peter Jung

Germany

Thomas Kaiser

Germany

Rajesh Khanna

India

David I. Laurenson

UK

Petri Mahonen

Germany

Montse Najar

Spain

Markus Rupp

Austria

Nikos C. Sagiias

Greece

Theodoros Tsiftsis

Greece

Laura Vanzago

Italy

Yang Xiao

USA

Guosen Yue

USA